Optimal amplification of the Crow instability

Vincent Brion, Denis Sipp, and Laurent Jacquin
Departement d'Aerodynamique Fondamentale et Experimentale, ONERA, 92190 Meudon, France

(Received 21 May 2007; accepted 31 August 2007; published online 26 November 2007)

A mechanism for promoting the Crow instability in a counter-rotating vortex pair is presented within the framework of linear dynamics. It consists of (i) the creation of a periodic array of vortex rings along the length of the vortices by stretching of vorticity at the leading hyperbolic point of the dipole, and (ii) the deformation of the vortices by the vortex rings leading to the Crow instability. A reduction of the characteristic time of the Crow instability by a factor of roughly 2 can be obtained by this mechanism. © *2007 American Institute of Physics*. [DOI: 10.1063/1.2793146]

Vortex hazard caused by aircraft trailing vortices has gained much attention during the past decades with the advent of jumbo jets. In certain situations, vortex wakes collapse through a chain process including deformation of columnar vortices by the Crow instability, vortex linking, and turbulence.[1] One way to alleviate vortex hazard is to accelerate the process by exciting the intrinsic instabilities of the wake. This is the idea developed in this article, in which we optimize the energy of the Crow perturbation by means of an appropriate initial perturbation. The growth rate of the Crow instability was first derived by Crow.[2] Vortices of the pair deform by mutual induction and oscillate in a plane inclined at approximately 45° about the horizontal. The oscillations grow exponentially in amplitude until the point when the two vortices touch, leading to final collapse. Several studies such as that of Crow and Bate[3] showed that exciting the vortex pair at the wavelength of the mutual induction instability could be efficient in accelerating the chain process. Other studies such as those of Crouch[4] and Fabre, Jacquin, and Loof[5] showed by a vortex filament method that systems of four vortices exhibit much larger amplification rates than the Crow instability. While these previous studies arbitrarily specify the structure of the perturbation as vortex filaments, in this article we use a global stability method based on a finite-element discretization with a high number of degrees of freedom that presupposes no particular shape for the initial perturbation. In the case of a single Lamb-Oseen vortex, Antkowiak and Brancher[6] and Pradeep and Hussain[7] have already reported that the optimal perturbation takes the form of spirals of vorticity outside the vortex core, which suggests that a similar mechanism of amplification can be expected in the case of the dipole as far as the two vortices are not too close to each other. Yet this suggestion is partially hindered by the presence of two hyperbolic stagnation points (hereafter simply referred to as hyperbolic points, "hyperbolic" standing for the hyperbolicity of the streamlines in the vicinity of these points, see Fig. 1) in the flow that are also known[8] to behave as energy amplifiers. The main objective of the study is to understand the roles that these two dynamics (that of the vortex and that of the hyperbolic point) play in the optimal amplification of the Crow instability.

Base flow. The basic flow is a two-dimensional pair of counter-rotating vortices symmetric with respect to $x=0$, which may[9] be characterized by the aspect ratio a/b of the dipole (see Fig. 1). Cartesian coordinates (x,y,z) are used throughout the study. Let us define S the computational domain, ∂S the far-field boundaries, and $S^+=S_{|x\geqslant 0}$ the right domain. These definitions allow us to define a as the radius of the vortices by $\Gamma a^2=\int\int_{S^+}\Omega_z\|\boldsymbol{x}-\boldsymbol{x_C}\|^2 dS$ with $\boldsymbol{x_C}=(x_C,y_C)=1/\Gamma\int\int_{S^+}\Omega_z \boldsymbol{x} dS$ the center of the right vortex, $\Gamma=\int\int_S^+\Omega_z dS$ its circulation, $b=2x_C$ the distance between the vortex centers, and Ω_z the axial basic vorticity. We consider a dipole at $a/b=0.2$ obtained by a two-dimensional direct numerical simulation (DNS) started with an initial dipole characterized by $a/b(t=0)=0.1$ and composed of two Lamb-Oseen vortices. This procedure produces a dipole that is a solution of the 2D incompressible steady Navier-Stokes equations (which is not the case initially) in the reference frame attached to the dipole (the pair drifts at a velocity of approximately $2\pi b/\Gamma$ under mutual velocity induction). The computational domain is S^+ and a symmetry boundary condition is used at the symmetry plane of the dipole to account for the left vortex. Streamlines of the flow are drawn in Fig. 1. During the simulation, the two vortices basically diffuse under the effect of viscosity with a viscous time scale $T_\nu=2\pi a^2/\nu$ and adapt under the strain mutually induced by one vortex onto the other. The time scale $T_{3D}=2\pi b^2/\Gamma$ of the three-dimensional perturbations is much smaller than T_ν, as $T_\nu/T_{3D}=\mathrm{Re}(a/b)^2$ and $\mathrm{Re}=\Gamma/\nu=3600$. The base flow can consequently be considered as quasisteady for the forthcoming stability analysis. We note $(\mathbf{U},P)$ the basic state (where $\mathbf{U}=(U,V,0)$), which is assumed homogeneous in the axial direction z. In the following, T_{3D} and b are used as reference time and length scales. Time $t=1$ is the time needed to have order 1 deformation of the vortices by the Crow instability.

Stability theory. In order to study the linear behavior of the dipole, we superimpose a small disturbance $\mathbf{q}=(\mathbf{u},p)$, where $\mathbf{u}=(u,v,w)$ onto the background flow $(\mathbf{U},P)$. Considering a Fourier decomposition of the form $\mathbf{q}(x,y,t)=(\tilde{u},\tilde{v},i\tilde{w},\tilde{p})(x,y,t)e^{ikz}+\mathrm{c.c.}$, where k is the axial wavenumber, the evolution of $\tilde{\mathbf{q}}=(\tilde{u},\tilde{v},\tilde{w},\tilde{p})$ is given by the initial value problem (1) derived from the incompressible Navier-Stokes equations linearized about the basic state $(\mathbf{U},P)$.

$$B\partial_t\tilde{\mathbf{q}}=A\tilde{\mathbf{q}},\quad \tilde{\mathbf{q}}(t=0)=\tilde{\mathbf{q}}_0,\quad \tilde{\mathbf{q}}_{|\partial S}=0, \tag{1}$$

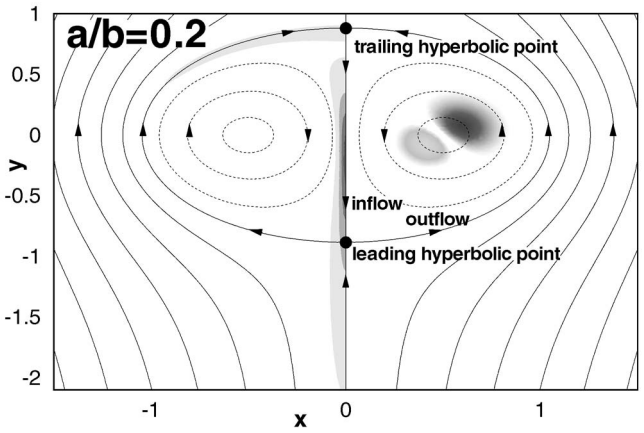

FIG. 1. Streamlines of the basic counter-rotating vortex pair (arrows indicate the direction of the flow). Right side: disturbance $\tilde{\omega}_z$ of the Crow mode at $k=0.9$. Left side: disturbance $\tilde{\omega}_x$ of the adjoint of the Crow mode. ω_z is odd and $\tilde{\omega}_x$ is even about the symmetry plane of the dipole. Note that the figure has been enlarged in the x direction for clarity.

$$A=\begin{pmatrix} -\partial_x U-\mathcal{C}+\mathcal{V} & -\partial_y U & 0 & -\partial_x \\ -\partial_x V & -\partial_y V-\mathcal{C}+\mathcal{V} & 0 & -\partial_y \\ 0 & 0 & -\mathcal{C}+\mathcal{V} & -k \\ \partial_x & \partial_y & -k & 0 \end{pmatrix}. \tag{2}$$

We noted $\mathcal{C}=U\partial_x+V\partial_y$ the convection of the perturbation by the base flow, $\mathcal{V}=2\pi/\mathrm{Re}(\partial_{xx}+\partial_{yy}-k^2)$ the viscous term, and $B=\mathrm{diag}(1,1,1,0)$. If we consider a normal mode decomposition of the form $\tilde{\mathbf{q}}(x,y,t)=\hat{\mathbf{q}}(x,y)e^{\sigma t}$ with $\sigma=\sigma_R+i\sigma_I$ a complex number, the equation yields the eigenproblem

$$A\hat{\mathbf{q}}=\sigma B\hat{\mathbf{q}}, \quad \hat{\mathbf{q}}_{|\partial S}=0. \tag{3}$$

The eigenmodes $\hat{\mathbf{q}}$ of the eigenproblem (3) are called direct modes. An adjoint problem can similarly be defined with a continuous adjoint operator A^+ given by the relation $(\tilde{\mathbf{q}}_1,A\tilde{\mathbf{q}}_2)=(A^+\tilde{\mathbf{q}}_1,\tilde{\mathbf{q}}_2)$ whatever $\tilde{\mathbf{q}}_{1,2}$ where the scalar product is given by $(\tilde{\mathbf{q}}_1,\tilde{\mathbf{q}}_2)=\int\int_S\tilde{\mathbf{q}}_1^*\cdot\tilde{\mathbf{q}}_2 dS$ and where * denotes the conjugate. The eigenmodes $\hat{\mathbf{q}}^+$ of A^+, called the adjoint modes, are solution of a generalized eigenproblem similar to (3) given by

$$A^+\hat{\mathbf{q}}^+=\sigma^+B\hat{\mathbf{q}}^+, \quad \hat{\mathbf{q}}^+_{|\partial S}=0, \tag{4}$$

$$A^+=\begin{pmatrix} -\partial_x U+\mathcal{C}+\mathcal{V} & -\partial_x V & 0 & \partial_x \\ -\partial_y U & -\partial_y V+\mathcal{C}+\mathcal{V} & 0 & \partial_y \\ 0 & 0 & \mathcal{C}+\mathcal{V} & k \\ \partial_x & \partial_y & -k & 0 \end{pmatrix}. \tag{5}$$

In comparison to the direct problem described by A, the convection in A^+ is reversed and the off-diagonal terms $-\partial_x V$ and $-\partial_y U$ are exchanged. Any direct mode has a corresponding adjoint mode and their eigenvalues are conjugate to each other.

A finite-element method with P2 space discretization for the velocity and P1 for the pressure is used to discretize the sparse matrices A, A^+, and B (size 5×10^5). Problems (3) and (4) are then solved by an Arnoldi method based on a shift and invert strategy (ARPACK package). The matrix inverse is solved thanks to a direct sparse LU solver (UMFPACK package). Once calculated, the direct and adjoint eigenmodes are normalized so that $(\hat{\mathbf{q}}_i,B\hat{\mathbf{q}}_i)=1$, $(\hat{\mathbf{q}}_i^+,B\hat{\mathbf{q}}_i)=1$, and the bi-orthogonality condition $(\hat{\mathbf{q}}_i^+,B\hat{\mathbf{q}}_j)=0$ if $i\neq j$ is verified.

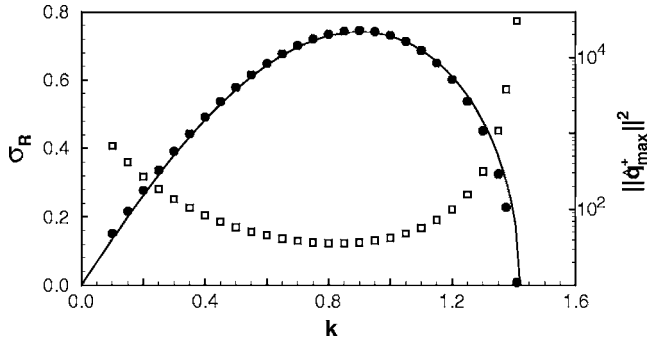

FIG. 2. Computed (filled points) growth rate σ_R of the Crow instability as a function of the axial wavenumber compared to the theory of Crow (line). Empty squares show the non-normal gain $\|\hat{\mathbf{q}}^+_{\max}\|^2$. Note that the Crow eigenmodes are nonoscillating ($\sigma_I=0$). Re=3600, $a/b=0.2$.

Energy gain. The dynamics of (1) will always be driven by the most unstable direct eigenmode at large time. It can be shown (see Schmid and Henningson[11]) that a specific initialization that consists in the adjoint mode $\hat{\mathbf{q}}^+_{\max}$ of the most unstable direct mode $\hat{\mathbf{q}}_{\max}$ will yield the perturbation with the maximum energy at large time. Defining the energy gain of a perturbation $\tilde{\mathbf{q}}(t)$ by

$$G(t)=\|\tilde{\mathbf{q}}(t)\|^2/\|\tilde{\mathbf{q}}(0)\|^2, \tag{6}$$

where the norm $\|\cdot\|$ is based on the scalar product $(\cdot,B\cdot)$, it may be shown that the maximum energy gain is $G_{\max}(t)=\|\hat{\mathbf{q}}^+_{\max}\|^2e^{2\sigma_{\max}t}$ obtained for $\tilde{\mathbf{q}}(0)=\hat{\mathbf{q}}^+_{\max}$. The non-normal gain $\|\hat{\mathbf{q}}^+_{\max}\|^2$ is the increase in amplification achieved by an initialization with the adjoint mode compared to an initialization with the direct mode.

Figure 2 reports the variation of the growth rate and the non-normal gain of the Crow instability with the wavenumber k. The most unstable Crow mode occurs for $k=0.9$. The related direct mode is depicted on the right side of Fig. 1 and the adjoint on the left side (the reason for showing $\hat{\omega}_x$ will be apparent later). The numerical code is validated against the theoretical inviscid growth rate given by Crow[2] and Saffman.[10] To our knowledge, this is the first time the growth rate of Crow has been calculated so successfully by a global method.

According to Fig. 2, the non-normal gain is greater as the growth rate is smaller. The minimum, which equals 36, is reached for the most unstable mode at $k=0.9$. This means that disturbing the dipole with the adjoint of the most unstable Crow mode gives an amplification 36 times greater at large time than a modal disturbance by the direct mode. The potential acceleration of the Crow instability related to this gain amounts to an interesting $\log(36)/(2\sigma_{\max})\simeq2.5$ time units. This non-normal gain can even be higher, i.e., 10^3 to 10^4 if the disturbance is chosen at a wavenumber k corre-

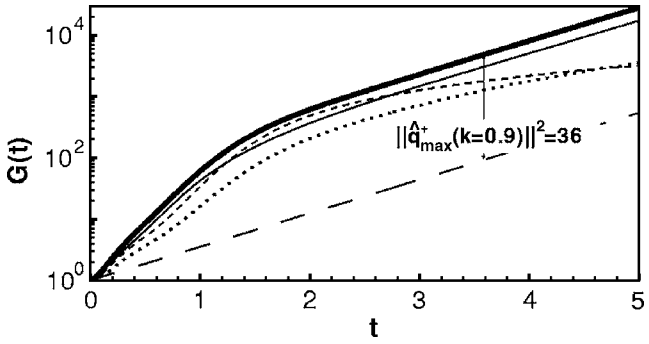

FIG. 3. Comparison between modal energy growth at $k=0.9$ (long dash), adjoint energy growth at $k=0.9$ (thick solid), energy growth induced by a perturbation (thin solid) containing $\tilde{\omega}_x$ on the symmetry axis, and most unstable perturbations at $k=0.2$ (short dash) and $k=1.4$ (dot). Re=3600, $a/b=0.2$.

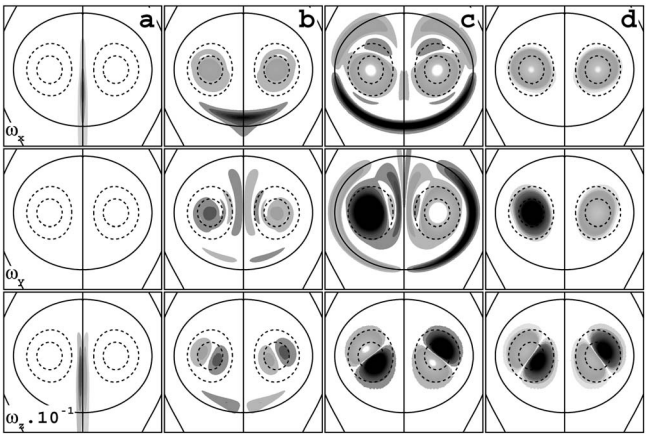

FIG. 4. Streamlines of the base flow and contours of perturbation vorticity through time evolution of the adjoint Crow mode [(a)–(c): $t=0.046;0.41;0.94$] at $k=0.9$. Column d represents the final Crow mode [(a)–(c) contour and (d) contour levels are different]. Contours (a)–(d) of $\tilde{\omega}_z$ are 10 times smaller than those of $\tilde{\omega}_x$ and $\tilde{\omega}_y$ to allow the use of the same contour levels. Re=3600, $a/b=0.2$.

sponding to lower growth rates. The influences of the Reynolds number and of the aspect ratio a/b of the dipole on the non-normal gain were also explored. Note that $\|\hat{q}^+_{max}\|^2$ increases slowly with Re ($\|\hat{q}^+_{max}\|^2=44$ for Re=9000) and decreases slowly with a/b ($\|\hat{q}^+_{max}\|^2=53$ for $a/b=0.17$). These results clearly state the high potential of the adjoint approach.

Linearized simulations. The sole value of the non-normal gain is not enough to conclude on the efficiency of the adjoint disturbance as the time needed to reach it is not known. Therefore, linearized simulations solving the problem (1) in time were launched with the different initializations evoked earlier (the legend refers to Fig. 3): the direct mode at $k=0.9$ (long dash), the adjoint mode at $k=0.9$ (thick solid), the adjoint at $k=0.2$ (short dash), and the adjoint at $k=1.4$ (dot) (note that the remaining curve is discussed at the end of the paper). The previously described finite-element method is used with a time discretization carried out by a second-order Lagrange-Galerkin method.

In Fig. 3, we see that the curve of the adjoint mode at $k=0.9$ reaches an asymptote parallel to the modal growth (a straight line in the log scale). This shows that after $t=1.5$, the adjoint perturbation has reached the direct modal structure and is amplified accordingly. The associated increase of amplification amounts to 36 as predicted by the non-normal gain, while in terms of time difference the value 2.5 obtained earlier is approximately recovered. This implies that once the transient period of amplification $t=1.5$ is over, the disturbance of the dipole by the adjoint perturbation provides an amplitude perturbation identical to that of the natural Crow instability on a time scale reduced by 2.5. Sparlart[1] and Crow and Bate[3] note a time period of 5 to 6 for the lifespan of trailing vortices. This means that a reduction of 2.5 shrinks by almost half this characteristic lifespan, which could be of great interest for the aeronautical industry. Energy amplification corresponding to initial perturbation by the adjoint modes at $k=0.2$ and 1.4 does not exhibit the expected strong energy gains quick enough, i.e., the transient period is greater than $t=5$. This renders these cases useless and justifies that we only focus on the case $k=0.9$ of the most unstable Crow mode.

Optimal mechanism. Figure 4 shows the steps leading to the optimal amplification of the Crow instability. The mechanism basically consists in amplification of $\tilde{\omega}_x$ at the leading hyperbolic point region (upper row, a-c) followed by the induction of the Crow instability in the vortex cores (lower row, c-d). As shown by Lagnado *et al.*,[8] transient energy growth at hyperbolic points occurs for initial vorticity parallel to the stretching direction. Indeed, at the leading hyperbolic point (Fig. 1), the equation for vorticity perturbation reduces to

$$\partial_t\tilde{\omega}_x=\gamma\tilde{\omega}_x+2\pi/\mathrm{Re}\Delta\tilde{\omega}_x, \tag{7}$$

$$\partial_t\tilde{\omega}_y=-\gamma\tilde{\omega}_y+2\pi/\mathrm{Re}\Delta\tilde{\omega}_y, \tag{8}$$

$$\partial_t\tilde{\omega}_z=2\pi/\mathrm{Re}\Delta\tilde{\omega}_z, \tag{9}$$

where $\gamma=\partial_x U=-\partial_y V\sim+1.7$ is the strain rate in the vicinity of the hyperbolic point. As a result, the initial perturbation with $\tilde{\omega}_x$ experiences a strong amplification as it passes in the vicinity of the leading hyperbolic point due to the stretching along the outflow streamline.

As the streamline bends up, $\tilde{\omega}_x$ is tilted (b) leading to the formation of $\tilde{\omega}_y$. Together $\tilde{\omega}_x$ and $\tilde{\omega}_y$ form a partial vortex ring around the dipole (c). This vortex ring creates axial and radial velocities within the dipole by the Biot Savart law and eventually induces axial vorticity in the regions where Ω_z is strong thanks to the production terms in the linearized equation of $\tilde{\omega}_z$

$$\partial_t\tilde{\omega}_z+\underbrace{U_\theta/r\partial_\theta\tilde{\omega}_z}_{\text{convection}}=\underbrace{-\tilde{u}_r\partial_r\Omega_z+k\Omega_z\tilde{u}_z}_{\text{production}}+\underbrace{\nu\Delta\tilde{\omega}_z}_{\text{diffusion}}. \tag{10}$$

As in the case of a single vortex,[6,7] the previous description of the optimal mechanism suggests that bending modes of the vortices are optimally induced by vortex rings that partially circle the rotational flow. Following this idea, the question of the optimal perturbation reduces to the question of

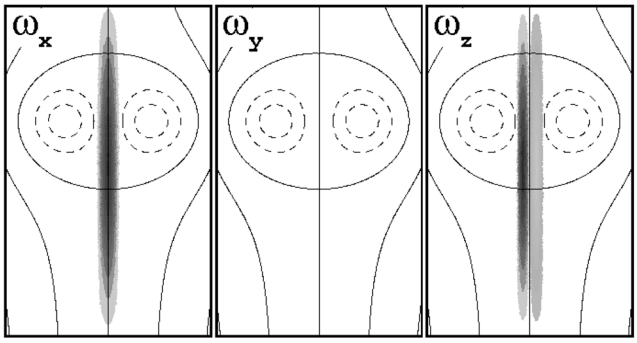

FIG. 5. Initial perturbation containing $\tilde{\omega}_x$ and $\tilde{\omega}_z$ and no $\tilde{\omega}_y$ at $k=0.9$. Note that $\tilde{\omega}_x$ also represents $\tilde{f}_y$ as $\tilde{\omega}_x=-\tilde{f}_y/k$.

how to optimally produce such partial vortex rings. While in the case of the single vortex it is the unrolling[6,7] of the spirals of vorticity around the vortex that forms them, in the case of the dipole, it is the leading hyperbolic point that plays that role. The results of these two configurations (dipole and single vortex) tend to suggest that the way to optimally disturb any compact distribution of vorticity is to create one or several partial vortex rings around it. Such a generalization could be investigated in a future study.

A question arises about the lack of a role for the trailing hyperbolic point. If it were to play a role, it would need an initial $\tilde{\omega}_y$ distribution located at its inflow streamline that would then be amplified along $x=0$ between the two vortices. But due to the symmetry of the perturbation, it appears that only the leading hyperbolic point can be efficiently used for vorticity stretching. Indeed, nonzero $\tilde{\omega}_x$ can be located on the stretching line of the leading hyperbolic point whereas $\tilde{\omega}_y$ being antisymmetric is zero on the stretching line of the trailing hyperbolic point. Moreover, because of the resultant dipolar distribution of $\tilde{\omega}_y$, only a weak velocity induction in the vortex core could take place, which would induce the Crow instability less efficiently.

Optimal forcing. While defining a practical method to trigger this amplification in real flows is beyond the scope of this article, it is still interesting to study theoretically the effect of control devices or background turbulence by modeling them by forces in the linearized equations. Solving an initial value problem initialized by $\tilde{\mathbf{q}}_0=(\tilde{\mathbf{u}}_0,\tilde{p}_0)$ is equivalent to applying a force $\tilde{\mathbf{F}}\delta(t)$ (δ is the Dirac function) to a flow field at rest.[10] Integrating the equation for the perturbation vorticity $\tilde{\boldsymbol{\omega}}$ over an infinitesimal time interval leads to $\tilde{\boldsymbol{\omega}}_0=\nabla\times\tilde{\mathbf{F}}$. The initial velocity field corresponding to the initial forcing is thus given by $\tilde{\mathbf{u}}_0=\tilde{\mathbf{F}}+\nabla\tilde{h}$, where $\tilde{h}$ satisfies a Poisson equation $\nabla\cdot\tilde{\mathbf{F}}=-\Delta\tilde{h}$ (with homogeneous Dirichlet boundary conditions on ∂S and a Neumann boundary condition on the symmetry plane) as $\nabla\cdot\tilde{\mathbf{u}}_0=0$. An initial perturbation can hence be interpreted in terms of a force acting initially in the momentum equation. As a result, the optimal perturbation is also to be interpreted as the optimal force for destabilizing the dipole. The control needed to have $\tilde{\omega}_x$ at the central plane of the dipole can consist in applying a vertical force $\tilde{\mathbf{F}}=(0,\tilde{f}_y,0)$ at the same location. This leads to $\tilde{\boldsymbol{\omega}}_0=(-k\tilde{f}_y,0,\partial_x\tilde{f}_y)$ as desired (no $\tilde{\omega}_y$). We chose an analytical expression for $\tilde{\mathbf{F}}$ with $\tilde{f}_y=(1+\cos(x/a_x))(1+\cos(y-y_0)/a_y)$ for $|x|\leqslant\pi a_x$ and $|y-y_0|\leqslant\pi a_y$ (y_0, a_x, and a_y, which control the location and the form of the distribution, are $y_0=-0.8$, $a_x=0.05$, and $a_y=0.7$ for $k=0.9$) and zero everywhere else, as shown in Fig. 5. The corresponding initial velocity field $\tilde{\mathbf{u}}_0$ is obtained by solving the preceding Poisson equation. Only 2% of the energy contained in $\tilde{\mathbf{F}}$ is lost in the projection process as $\|\tilde{\mathbf{u}}_0\|/\|\tilde{\mathbf{F}}\|=0.98$ ($\|\tilde{\mathbf{F}}\|=\int_S(\tilde{f}_x^2+\tilde{f}_y^2+\tilde{f}_z^2)dS$). Figure 3 shows the gain in energy obtained by this forcing (thin solid line) and it is clear that the amplification, though not optimal, is significant. A similar perturbation with initial $\tilde{\omega}_y$ and $\tilde{\omega}_z$ and no $\tilde{\omega}_x$ (generated by $\tilde{f}_x$ instead of $\tilde{f}_y$) leads to no nonnormal gain (not shown here). This confirms the physical mechanism involving $\tilde{\omega}_x$ as a necessary ingredient for optimal destabilization of the dipole and the fact that it is possible to create this quasi-optimal perturbation with a force having a simple distribution. These results clearly open new perspectives and challenges for controlling vortex pairs in real flows.

[1] P. R. Spalart, "Airplane trailing vortices," Annu. Rev. Fluid Mech. **30**, 107 (1998).
[2] S. C. Crow, "Stability theory for a pair of trailing vortices," AIAA J. **8**, 2172 (1970).
[3] S. C. Crow and E. R. Bate, Jr., "Lifespan of vortices in a turbulent atmosphere," J. Aircr. **13**, 476 (1976).
[4] J. Crouch, "Instability and transient growth for two trailing vortex pairs," J. Fluid Mech. **350**, 311 (1997).
[5] D. Fabre, L. Jacquin, and A. Loof, "Optimal perturbations in a four-vortex aircraft wake in counter-rotating configuration," J. Fluid Mech. **451**, 319 (2002).
[6] A. Antkowiak and P. Brancher, "Transient energy growth for the Lamb-Oseen vortex," Phys. Fluids **16**, L1 (2004).
[7] D. S. Pradeep and F. Hussain, "Transient growth of perturbation in a vortex column," J. Fluid Mech. **550**, 251 (2006).
[8] R. R. Lagnado, N. Phan-Thien, and L. G. Leal, "The stability of two-dimensional linear flows," Phys. Fluids **27**, 1094 (1983).
[9] D. Sipp, L. Jacquin, and C. Cossu, "Self-adaptation and viscous selection in concentrated 2D vortex dipoles," Phys. Fluids **12**, 245 (2000).
[10] P. G. Saffman, *Vortex Dynamics* (Cambridge University Press, Cambridge, UK, 1992).
[11] P. J. Schmid and D. S. Henningson, *Stability and Transition in Shear Flows*, Applied Mathematical Sciences Vol. 142 (Springer, New York, 2002).